Journal of Building Engineering 28 (2020) 101092

Contents lists available at ScienceDirect

Journal of Building Engineering

journal homepage: http://www.elsevier.com/locate/jobe

Constitutive models for nonlinear analysis of SFRC corbels

F.B.A. Beshara [a], T.S. Mustafa [a,*], A.A. Mahmoud [a,b], M.M.A. Khalil [a]

[a] Civil Engineering Dept., Faculty of Engineering, Shoubra, Benha University, Egypt
[b] Higher Institute of Engineering, 15 May, Egypt

ARTICLE INFO

Keywords:
Corbels
Steel fiber reinforced concrete
Nonlinear finite element
Shear capacity
Load-deflection curves
Load-steel strain curves

ABSTRACT

In this paper, nonlinear constitutive models are proposed for steel fiber reinforced concrete (SFRC) in compression and tension. The models were implemented in the finite element computer program ANSYS for 3-D nonlinear analysis of SFRC corbels under monotonic static loading. Several validation studies have been performed for normal-strength and high-strength SFRC corbels with constant or variable depth. Good agreement is generally achieved between experimental and numerical results for the load-deflection curves and crack patterns. Additionally, parametric studies have been performed in order to investigate the effect of structural parameters on the performance of SFRC corbels. It was found that: (1) increasing the concrete compressive strength (f_c') improves corbel shear capacity and toughness, (2) the inclusion of steel fiber (V_f) delays premature shear failure for corbels and enhances strain ductility, (3) an enhancement in shear capacity and strain ductility is noticed by increasing the ratio of horizontal stirrups (ρ_h), and finally, (4) increasing the shear span-to-depth ratio (a/d) reduces the shear capacity of SFRC corbels. Corbel shear capacity increases by 27% due to a 33% increase in (f_c'), by 31% due to $V_f = 1\%$ inclusion, by 20% due to a 1% increase in (ρ_h), and by 20% due to a 39% decrease in (a/d) ratio. The proposed nonlinear finite element approach is efficient in determining the expected enhancement in shear capacity and ductility of SFRC corbels, and consequently in optimizing design parameters for such elements.

1. Introduction

Corbels are short cantilever members that project from a column or a wall to support another beam or heavy concentrated load. The importance of these members is clear in precast buildings where corbels support beams and girders. Corbels are characterized by a shear span-to-depth ratio (a/d) lower than unity. Over the years, the contribution of steel fibers on the structural behaviour of concrete corbels has been experimentally studied [1–10]. Based on the main findings from the literature, it was found that steel fibers inclusion enhances the shear capacity of corbels, and can replace partially or fully the stirrups [11]. In addition, using steel fibres improves the ductility and toughness of the reinforced concrete corbels [12]. Theoretical studies using the nonlinear finite element (FE) for modelling corbels have been idealized using several software packages such as ATENA, ANSYS and LUSAS computer programs [13–16].

Numerical predictions with the aim of the FE analysis should be provided on SFRC corbels for better evaluation of the experimental results. Accordingly, constitutive modelling for SFRC in compression and tension are adopted [17] in this study. Validation studies for the adopted model are provided by applying the finite element model to predict the behaviour of SFRC corbels that were experimentally tested in the literature [1–4]. Based on the good agreement that have been achieved between the numerical models and the experimental results, parametric studies have been performed to investigate the effect of different structural factors on the response of SFRC corbels. The main studied parameters herein include: (1) the effect of concrete strength (f_c'), (2) fiber volume (V_f), (3) fiber aspect ratio (l_f/φ_f), (4) horizontal stirrups ratio (ρ_h) and (5) shear span-to-depth ratio (a/d). For each parameter, the predicted response curves are plotted and analyzed.

2. Modelling of SFRC corbels

2.1. Finite element geometric idealization

The finite element modelling and nonlinear analysis is performed using ANSYS software [18]. The structural element types used for geometric idealization of the different materials are Solid 65 for non-fibrous

* Corresponding author.
E-mail address: dr_tareksayedm@yahoo.com (T.S. Mustafa).

https://doi.org/10.1016/j.jobe.2019.101092
Received 16 July 2019; Received in revised form 22 November 2019; Accepted 25 November 2019
Available online 27 November 2019

Fig. 1. Structural elements idealization for the numerical models [18].

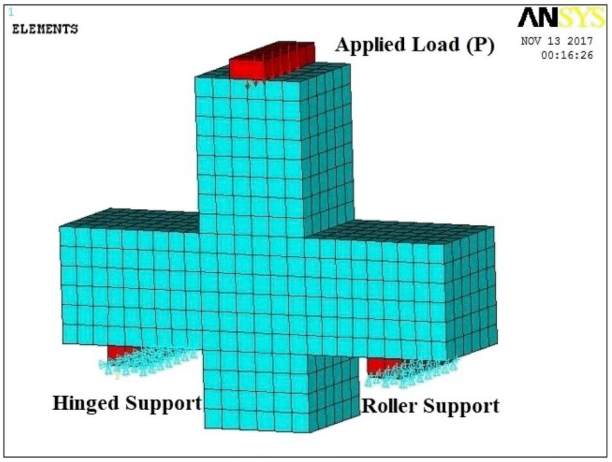

Fig. 2. The applied Load and the Support Conditions of the Corbels [17].

& fibrous concrete, and link 8 for steel bars & stirrups. In order to avoid stress concentration problems such as localized crushing of concrete elements near the bearing and loading plates, steel plates with 25 mm thickness are modelled by SOLID 45 at the location of supports and loading locations in SFRC corbels. The structural element types used to discrete the different materials are presented in Fig. 1.

In order to solve the nonlinear analysis equations of corbels, Newton-Raphson equilibrium iteration technique is used in the ANSYS software. This technique is based on a series of successive linear approximations with corrections. In this study, the convergence criterion is based on a displacement control. The infinite norm of displacement and the convergence precision is 0.05 [18]. In order to improve the convergence of nonlinear analysis, adaptive descend gene, linear searching, forecasting and dichotomy was used at the same time.

The displacement boundary conditions are required to constrain the models. To simulate the hinged support boundary condition of the corbel, the translations at the nodes (U_X, U_Y and U_Z) are assigned as a constant value of zero while the other support is simulated as roller by assigning the translations at the nodes (U_Y) equal zero value. The force (P) is applied at the top of columns segment in the gravity direction to simulate the experimentally tested corbels. The load is applied as incremental loads. Adjustment is set for each increment to reach results at certain specific load level. Fig. 2 clarifies the applied load and the supports conditions of the corbels. The maximum number of iterations in each load step is set as program default.

2.2. Constitutive modelling for fibrous concrete in compression

The constitutive modelling for fibrous and non-fibrous concrete in compression is adopted by Hognestad-Popvics stress-strain curve [19]. As shown in Fig. 3, the curve consists of two branches, the first branch represents the ascending one until the peak stress (f_p) and the corresponding strain (ε_p) are reached. It is defined by:

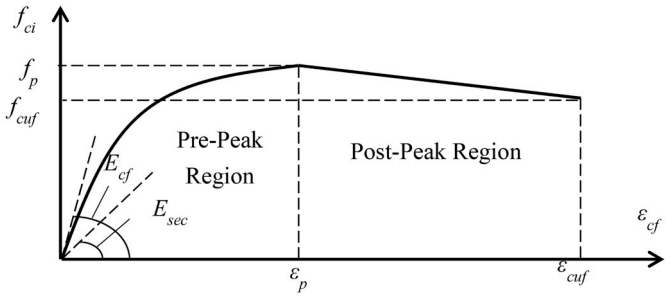

Fig. 3. Hognestad-Popvics stress-strain curve for concrete in compression [19].

$$f_{ci} = f_p\left(2\left(\frac{\varepsilon_{ci}}{\varepsilon_p}\right) - \left(\frac{\varepsilon_{ci}}{\varepsilon_p}\right)^2\right) \quad (1)$$

Where:

f_p = the peak compressive stress; determined experimentally from standard specimens;
ε_p = the concrete compressive strain corresponding to f_p;
f_{ci} = the concrete compressive stress corresponding to concrete compressive strain ε_{ci};
ε_{ci} = the concrete compressive strain corresponding to concrete compressive stress f_{ci}.

The second branch represents the descending branch (post peak) in which the curve descends into a softening region till the ultimate strain (ε_{cuf}) and crushing failure occurs [19]. The stress strain curve for this branch is defined by:

$$f_{ci} = f_p\frac{n\left(\frac{\varepsilon_{ci}}{\varepsilon_p}\right)}{n - 1 + \left(\frac{\varepsilon_{ci}}{\varepsilon_p}\right)^n} \quad (2)$$

$$n = \left(\frac{E_c}{E_c - \mathrm{E}_{Sec}}\right) \quad (3)$$

Where:

E_c = the initial tangent modulus for non-fibrous concrete in MPa and is defined according to ACI-318 14 [20] by the following equations:

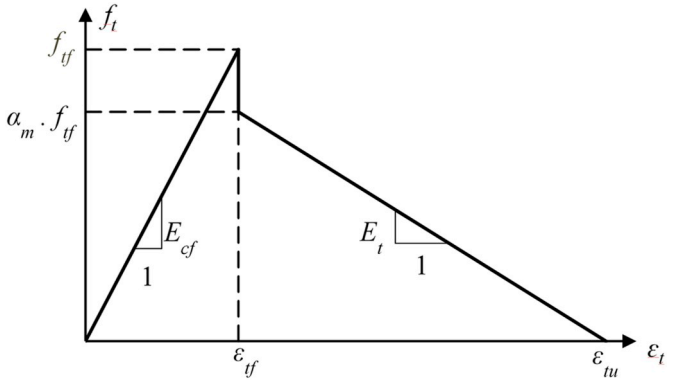

Fig. 4. Stress-strain curve for concrete in tension [21].

$$E_c = 4700\sqrt{f_c'} \tag{4}$$

f_c' = the concrete compressive strength of non-fibrous concrete in MPa

E_{sec} = the secant modulus at peak stress in MPa and is defined as:

$$E_{Sec} = \left(\frac{f_p}{\varepsilon_p}\right) \tag{5}$$

For the constitutive modelling of SFRC in compression, some modifications in the mechanical properties for concrete are applied. The initial tangent modulus (E_{cf}), and the ultimate compressive strain (ε_{cuf}) are estimated [21] as:

$$E_{cf} = 5000\sqrt{f_{cf}'} \tag{6}$$

$$\varepsilon_{cuf} = 0.0021 + 0.007\frac{V_f\, l_f}{\varphi_f} \tag{7}$$

Where:

V_f = volume fraction of the steel fiber;
l_f = length of the steel fiber;
φ_f = diameter of the steel fiber;

Furthermore, the compressive strength of non-fibrous concrete (f_c') is slightly increasing to (f_{cf}') (in MPa) [22] as:

$$f_{cf}' = f_c'\left(1 + 0.1066\frac{V_f\, l_f}{\varphi_f}\right) \tag{8}$$

2.3. Constitutive modelling of fibrous concrete in tension

Linear-tension softening stress-strain curve is modified and used in modelling fibrous concrete in tension. As shown in Fig. 4, the curve consists of two branches, the first branch represents the ascending one in which the relationship between stress and strain diagram is assumed to be linear till the tensile strength of concrete (f_{tf}) is reached [21]. The corresponding strain (ε_{tf}) to the peak stress (f_{tf}) which indicates the appearance of the crack initiation is defined as:

$$\varepsilon_{tf} = \frac{f_{tf}}{E_{cf}} \tag{9}$$

To take into consideration the contribution of steel fiber into plain concrete, the following equation defines the relation between the tensile strength of SFRC composite (f_{tf}) and non-fibrous composite (f_t) in terms of fiber parameters [21]:

$$f_{tf} = f_t\left(1 - V_f\right) + 0.45\, F\sqrt{f_{cf}'} \tag{10}$$

$$F = V_f\,\frac{l_f}{\varphi_f}\,\lambda \tag{11}$$

Where:

F = fiber reinforcing index [23].
λ = factor depends on the shape of steel fibers defined as 1.0 in case of hooked end steel fiber and as 0.50 in case of straight steel fiber [24].

After the crack initiation, the behavior of concrete cracks is represented by a smeared model. The cracked concrete can sustain some tensile stresses perpendicular to the crack by the tension stiffening. To consider the pullout resistance of fibrous concrete, the tension stiffening factor (α_m) is represented by Ref. [24]:

$$\alpha_m = \frac{O_{pc}'}{f_{tf}} \tag{12}$$

Where:

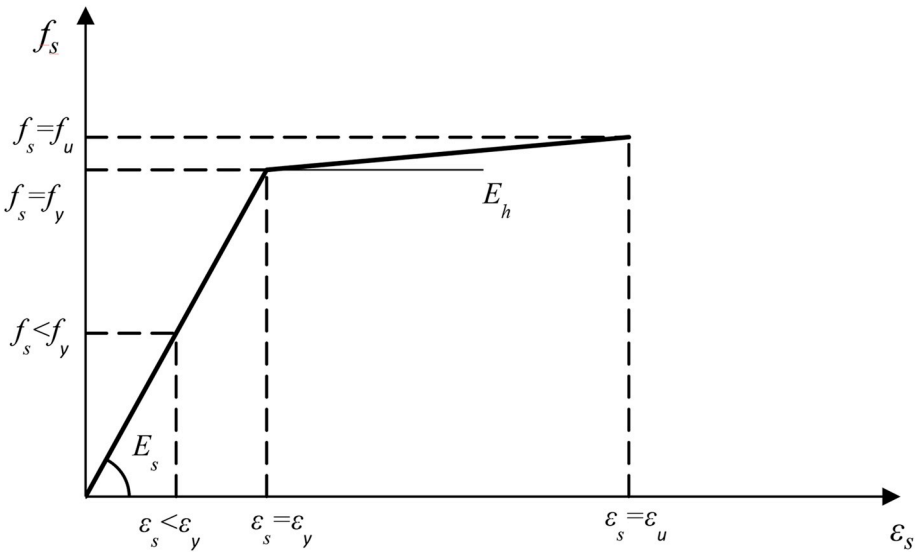

Fig. 5. Bilinear Stress-Strain Curve for the Steel reinforcement Modelling [26].

Table 1
Basic mechanical properties of specimens of validation studies.

Ref.	Corbel	f_p Mpa	f_{tf} Mpa	ε_{cu}	$\rho_s = A_s/(bd)\%$	f_y Mpa	$\rho_h = A_h/(bd)\%$	f_{yh} Mpa	V_f %	$\frac{l_f}{\varphi_f}$	b x d (mm)	a (mm)
[1]	SP.23	27	5.12	0.00236	1.0	452	–	–	2.0	60	150 × 135	110
	SP.37	30.3	5.72	0.0032	1.5	452	–	–	2.0	60	150 × 135	135
[2]	A2	48.5	3.59	0.0035	0.613	488	1.77	445	–	–	160 × 145	130
	A3	52.9	4.77	0.0048	0.613	488	–	–	1.0	60	160 × 145	130
[3]	C2	33.75	3.4	0.0029	0.95	491	–	–	–	–	150 × 235	100
	C4	34.75	3.5	0.00295	0.95	491	–	–	0.4	80	150 × 235	100
[4]	C1-SF	70.2	7.3	0.0038	0.55	490	1.19	490	0.75	50	600 × 575	175
	C2-SF	70.2	7.3	0.0038	0.55	490	1.19	490	0.75	50	600 × 575	175

Where:
b = the corbel width (mm).
d = the effective beam depth = total beam depth-concrete cover (mm).
a = the shear span length (mm).
A_s = the area of the main tension steel reinforcement (mm^2).
A_h = the area of the horizontal stirrups branches (2 branches) (mm^2).
S = the spacing of the horizontal stirrups (mm).
f_{yh} = the yield stress of the horizontal stirrups (MPa).

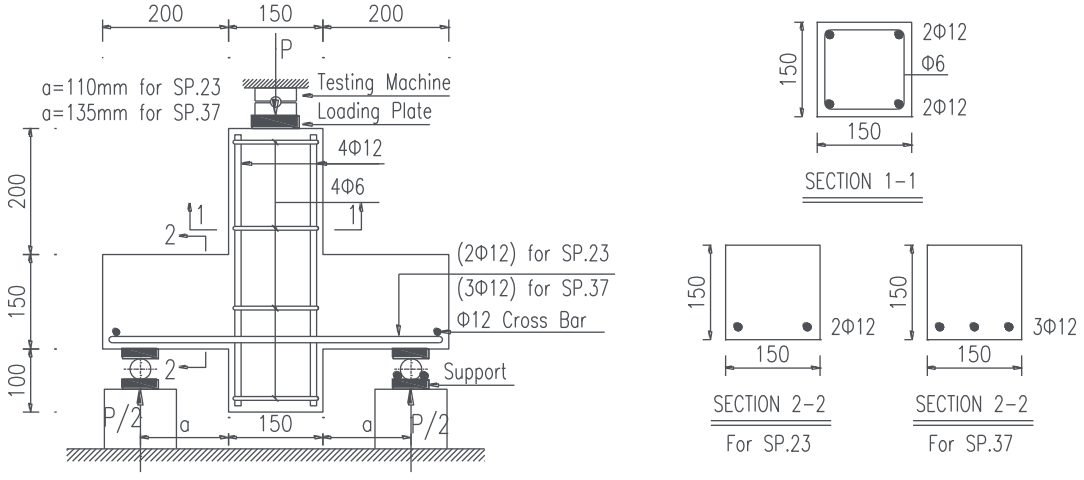

(a) Corbels (SP.23) and (SP.37) [1]

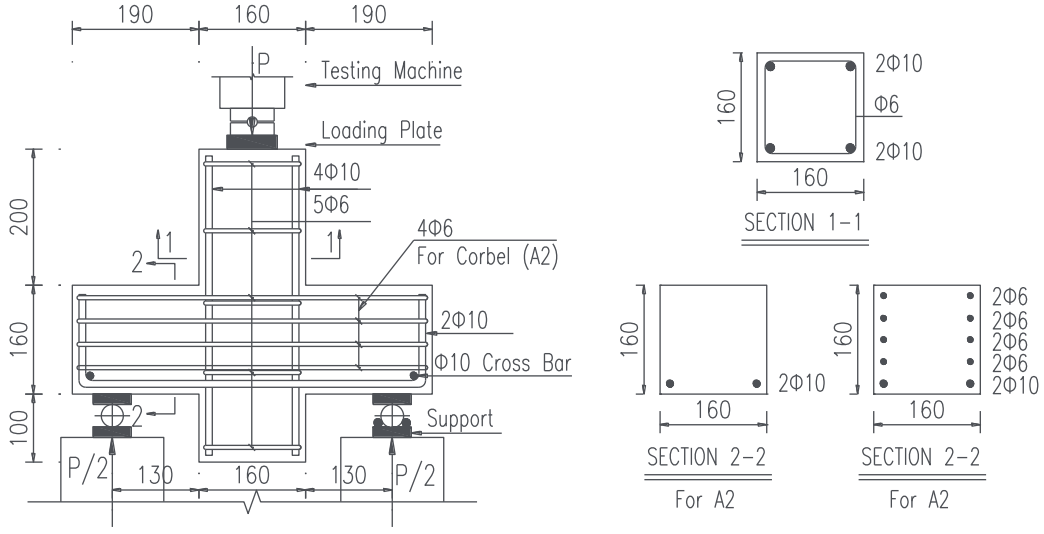

(b) Corbels (A2) and (A3) [a‡av

Fig. 6. Details of the Tested Corbels with constant depth.

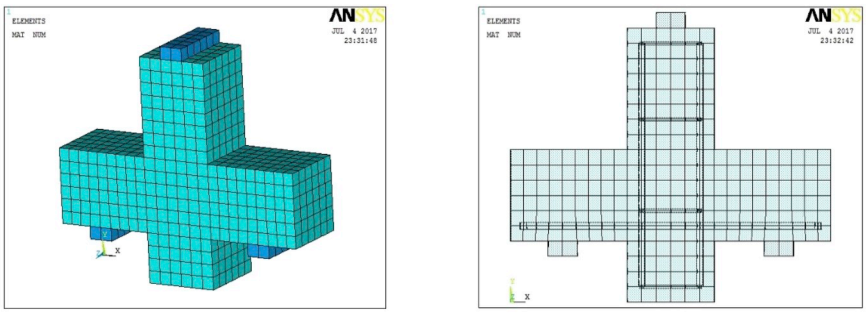

(a) Finite Element Models for Corbels (SP.23) and (SP.37)

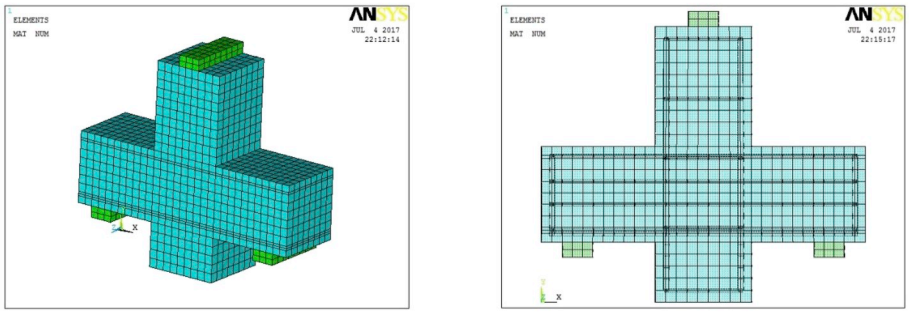

(b) Finite Element Models for Corbel (A2)

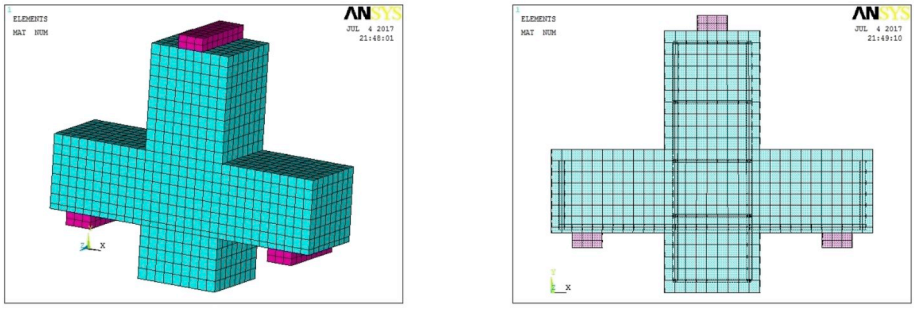

(c) Finite Element Models for Corbel (A3)

Fig. 7. Finite Element Simulation Models for the Corbels with constant depth.

O'_{pc} = the post cracking strength of SFRC (in MPa), and can be defined as [25]:

$$O'_{pc} = 0.2872\, F\, (f_{cf}')^{\frac{2}{3}} \tag{13}$$

In this study, the maximum value for the tension stiffening factor (α_m) is taken as 0.6. The second branch of the tensile stress strain curve represents the descending one which represents the tension stiffening area. The value of the ultimate strain (ε_{tu}) at which the tensile stress reduces to zero [24] is defined as:

$$\varepsilon_{tu} = 6\ \varepsilon_{tf} \tag{14}$$

2.4. Constitutive modelling of steel reinforcement

Bilinear stress-strain curve is used to idealize the behavior of the steel bars. As shown in Fig. 5, the stress-strain curve consists of two straight branches; the first branch represents the ascending branch at which the steel strain (ε_s) and the steel stress (f_s) are linearly increased up to the yield strain (ε_y) and the yield stress (f_y) respectively. The modulus of elasticity for the steel reinforcement is denoted by (E_s). The relationship for the two straight lines is expressed through the following equations [26]:

$$f_s = E_s\, \varepsilon_s \qquad \varepsilon_s \leq \varepsilon_y \tag{15a}$$

$$f_s = f_y + E_h\, (\varepsilon_s - \varepsilon_y) \qquad \varepsilon_s > \varepsilon_y \tag{15b}$$

Where;

ε_u = the ultimate strain of the steel reinforcement = 10 ε_y;
f_u = the ultimate stress of the steel reinforcement corresponding to the ultimate strain ε_u;
E_s = the modulus of elasticity of the reinforcing steel (2×10^5 MPa);
E_h = the modulus of elasticity at the second branch of the curve that describes the strain hardening region. E_h can be considered as [26]:

$$E_h = 0.1\, E_s \tag{16}$$

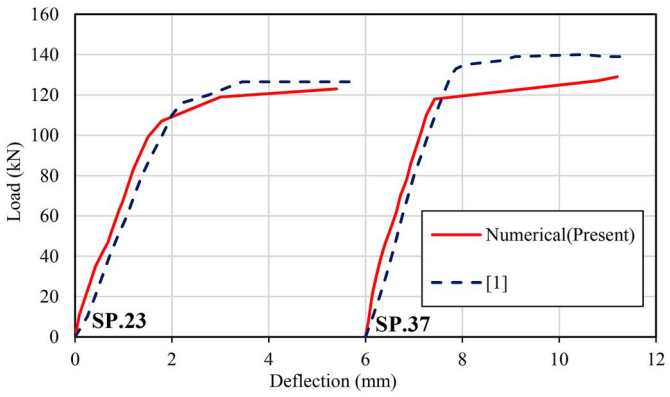

(a) Load-Deflection Curves for Corbels (SP.23) and (SP.37)

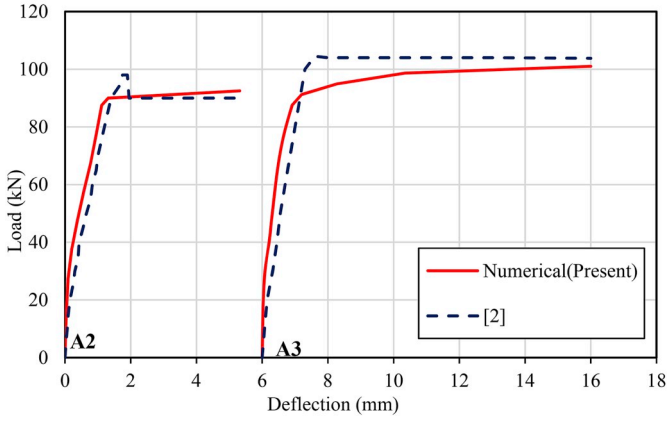

(b) Load-Deflection Curves for Corbels (A2) and (A3)

Fig. 8. Predicted and Measured Load-Deflections curves of Corbels with Constant Depth.

3. Validation studies

Validation studies are presented for several SFRC corbels. Table 1 presents summary for the geometrical and mechanical properties of the validated specimens.

3.1. SFRC corbels with constant depth

Two verification studies are considered for SFRC corbels with constant depth. The first case study includes two Normal-strength SFRC (NSSFRC) corbels, namely (SP.23) and (SP.37), which were experimentally tested in Ref. [1]. In the second case study, two high-strength SFRC (HSSFRC) corbels are chosen and are denoted by (A2) and (A3) in the experimental program [2]. The geometrical and material details are shown in Table 1. The details of the tested corbels [1,2] are presented in Fig. 6. Also, the finite element simulation models are shown in Fig. 7 for the corbels with constant depth.

3.1.1. Load-deflection curves

Based on the load-deflection curve, beneficial results are obtained such as: (1) the ultimate load carrying capacity (P_u), (2) the corresponding ultimate deflection (Δ_u), (3) the load at yield point (P_y) and (4) the corresponding deflection (Δ_y). Finally, area under the load–deflection curve which describes the toughness (I) is calculated. Fig. 8 presents the predicted numerical results with the experimental results for all corbels with constant depth. The figure shows a good agreement between the experimental results [1] and the predicted results at different response levels. The following findings can be concluded from the figure:

1. At the ultimate level, the average ratio [$(P_{u,\ (EXP)})/P_{u,\ (FE)}$] for the four corbels is 1.06. The average value of ultimate deflection ratio [$(\Delta_{u\ (EXP.)})/(\Delta_{u\ (FE)})$] is 1.04.
2. At the yield level, the average ratio [$(P_{y,\ (EXP)})/P_{y,\ (FE)}$] for all corbels is 1.07. Also, the average yield deflection ratio [$(\Delta_{y\ (EXP)})/(\Delta_{y\ (FE)})$] is 1.13.
3. The average toughness ratio [$(I_{\ (EXP)}/I_{\ (FE)}$] for the four corbels is 1.02.
4. All specimens failed in flexure and appeared to behave in an elastic-plastic manner, indicating yielding of main bars before reaching the maximum load. Also, fibers inclusion improves the confinement of the compression zone of corbel.
5. Compared with the non-fibrous corbel A2, the complete flexural capacity of fibrous corbels was reached and ductile behaviour was predicted. This circumstance highlights the effectiveness of fibers as shear reinforcement.

3.1.2. Crack pattern and failure mode

Comparison between the experimental crack patterns versus the predicted crack patterns for NSSFRC and HSSFRC corbels are shown in Fig. 9. As shown in the figure, good agreement is noticed between the experimental and the numerical crack patterns. For all fibrous specimens, the predicted failure mode is flexural mode. The failure mode is characterized by wide flexural vertical cracks occurring close to the column-corbel intersection after extensive yielding of main steel bars. Also, the figure indicates that the mode failure was changed from being diagonal splitting for non-fibrous corbel A2 to ductile flexure, as in the case of fibrous corbels SP.23, SP.37 and A3.

3.2. SFRC corbels with variable depth

For SFRC corbels with variable depth, two verification studies are considered. The first case study represents two NSSFRC corbels which were experimentally tested [3] and labelled by (C2) and (C4). In the second case study, two full-scale HSSFRC specimens; (C1-SF) and (C2-SF), published in (2004) [4] were chosen to verify the analysis output of ANSYS. The geometrical and material details are shown in Table 1. Specimen (C1-SF) is subjected to vertical load (P) which acts on the top of column only. On the other hand, specimen (C2-SF) is subjected to vertical load (P) at the top of the column and horizontal load (N_H) at the bottom of corbels. The value of (N_H) is 20% of the vertical load on each side of the specimen. The details of the tested corbels [3,4] are presented in Fig. 10. Also, the finite element simulation models are shown in Fig. 11.

3.2.1. Load-deflection relationship

The experimental and the predicted load-deflection curves are plotted for corbels C2, C4, (C1-SF), and (C2-SF) in Fig. 12. The figure shows good agreement between the experimental and the predicted results at different response stages. The following conclusions are drawn from the study of the figure:

1. At the ultimate level, the average load ratio [$P_{u\ (EXP)}/P_{u\ (FE)}$] is 0.97 for the four corbels. Also, the average value of ultimate deflection ratio [$\Delta_{u\ (EXP)}/\Delta_{u\ (FE)}$] is 0.96
2. At the yield level, the average ratios of the experimental and the predicted values; [$P_{y\ (EXP)}/P_{y\ (FE)}$] and [$\Delta_{y\ (EXP)}/\Delta_{y\ (FE)}$] are respectively 0.94 and 1.02.
3. Toughness (I) for the experimental works and the predicted numerical models are close. The ratio [I_{EXP}/I_{FE}] for the four corbels is 0.96.
4. For corbels C2 and C4 with constant (a/d) ratio, the inclusion of steel fibers leads to an increase in the ultimate shear capacity, and to a decrease in the deflection values at same loading level.

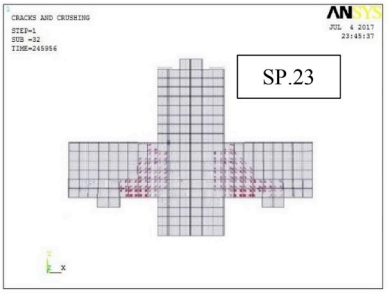

(a) SP. 23 - Predicted Crack Pattern

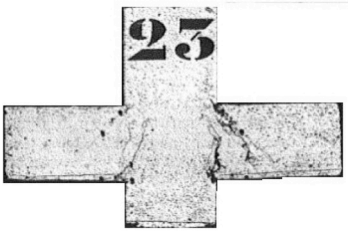

(b) SP. 23 - experimental Crack Pattern

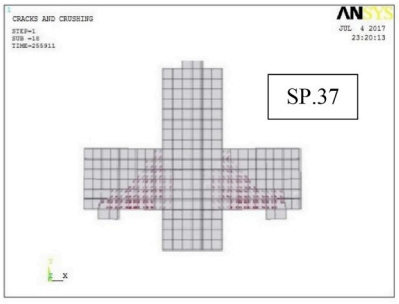

(c) SP. 37 - Predicted Crack Pattern

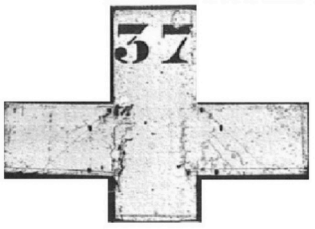

(d) SP. 37 - experimental Crack Pattern

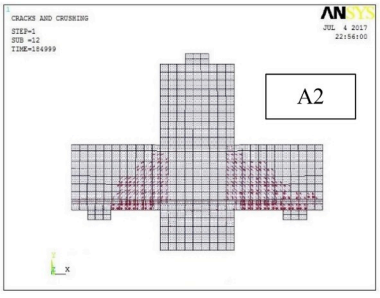

(e) A2 - Predicted Crack Pattern

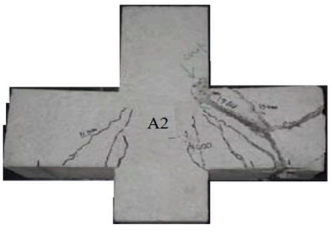

(f) A2 - experimental Crack Pattern

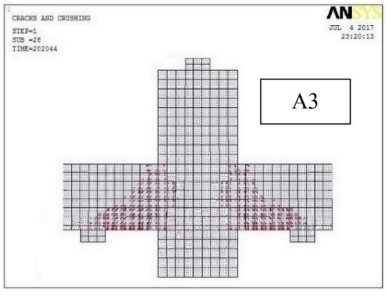

(g) A3 - Predicted Crack Pattern

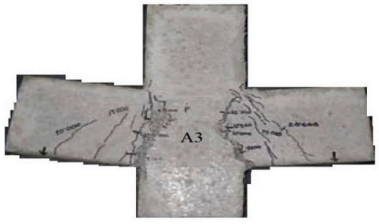

(h) A3 - experimental Crack Pattern

Fig. 9. Predicted & observed cracking patterns for corbels with constant depth.

5. For corbels C1-SF ($N_H = 0.0$) and C2-SF ($N_H = 0.2$), the existence of horizontal load at the corbel end decreases the vertical load capacity by 25% of SFRC corbel.

3.2.2. *Crack pattern and failure mode*

As shown in Fig. 13, good agreement is noticed between the experimental and the predicted crack patterns for corbels C2 and C4. The failure mode for corbels C2 and C4 is diagonal splitting of concrete. The diagonal splitting is described by diagonal cracks extending from the top of the column-corbel junction toward the bearing plate. Also, the figure indicates that the presence of steel fibers delays the initiation and propagation of concrete cracks due to the dowel resistance of fibers. However, the use of small fiber content (0.4%) does not change the brittle failure mode to ductile one. For corbels C1-SF and C2-SF, the cracking patterns were not given [4].

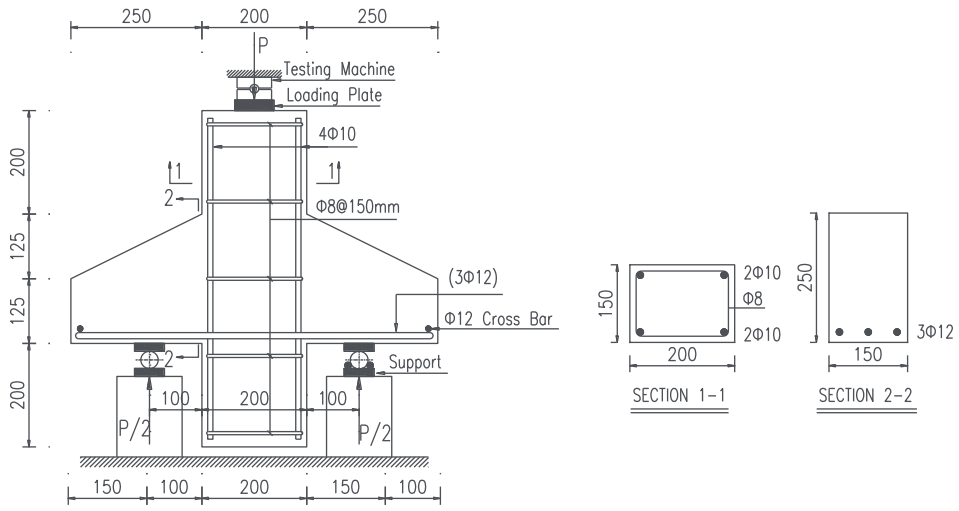

(a) Corbels (C2) and (C4) [3]

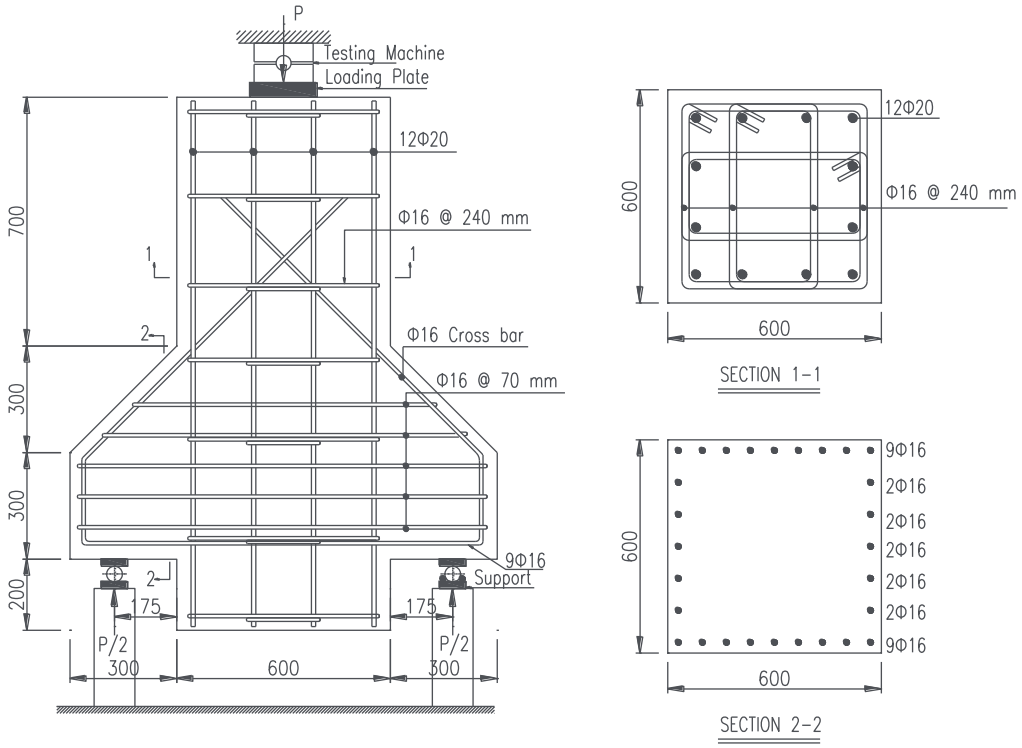

(b) Corbels (C1-SF) and (C2-SF) [4]

Fig. 10. Details of the Tested Corbels with variable depth.

3.3. Overall evaluation of validation studies

Table 2 presents summary of the results obtained from the experimental works [1–4] with the non-linear finite element analysis (NLFEA) models by ANSYS computer program. For all studied cases, good correlation is noticed from the comparison between the experimental and the predicted results which include the load-deflection curves and crack patterns. At yield level, the overall average value for [$P_{y\ (EXP)}/P_{y(FE)}$] ratio and [$\Delta_{y\ (EXP)}/\Delta_{y\ (FE)}$] ratio for all specimens are 1.01 and 1.08 respectively. At the ultimate level, the overall average value for [$P_{u\ (EXP)}/P_{u\ (FE)}$] ratio and [$\Delta_{u\ (EXP)}/\Delta_{u\ (FE)}$] ratio for all specimens are 1.02 and 1.03 respectively. Accordingly, ANSYS computer program on joint with the proposed constitutive models is a good tool for modelling fibrous and non-fibrous concrete corbels with and without horizontal stirrups, with different material parameters, shapes and the applied loads.

4. Parametric studies

In order to investigate the effect of different parameters on the structural response; series of SFRC corbels, which labelled with (S1, S2... S15) are analyzed. As given in Table 3, the main parameters studied herein include: (1) the concrete strength (f_c'), (2) volume of fibers (V_f), (3) fiber aspect ratio (l_f/φ_f) where l_f *and* φ_f are respectively fiber length

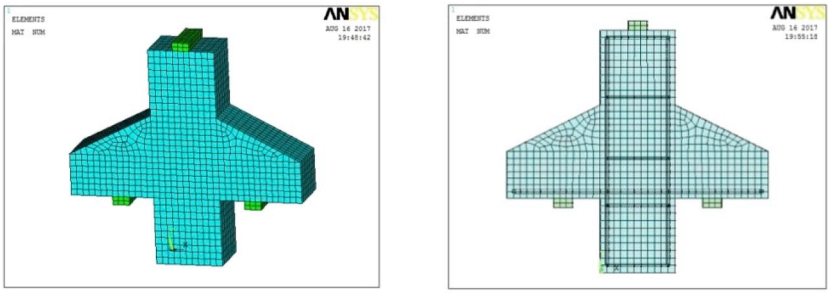

(a) Finite Element Models for Corbels (C2) and (C4)

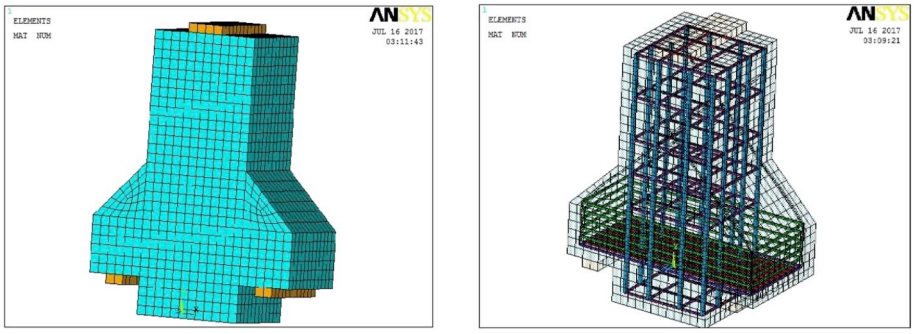

(b) Finite Element Models for Corbels (C2) and (C4)

Fig. 11. Finite Element Simulation Models for the Corbels with variable depth.

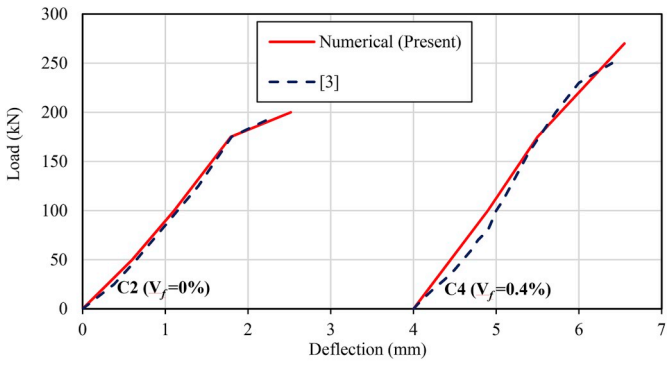

(a) Load-Deflection Curves for Corbels (C2) and (C4)

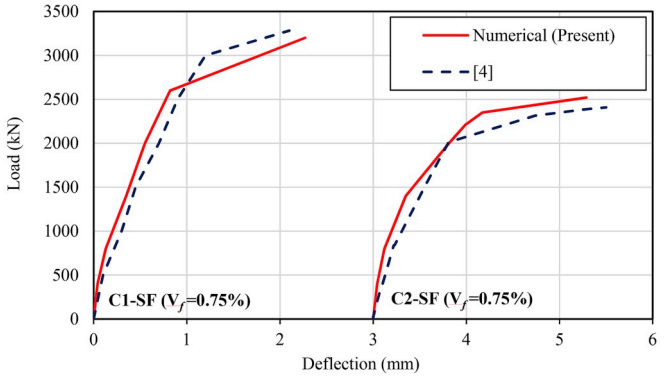

(b) Load-Deflection Curves for Corbels (C1-SF) and (C2-SF)

Fig. 12. Predicted and Measured Load-Deflections curves of Corbels with variable depth.

and diameter, (4) ratio of horizontal stirrups (ρ_h) and (5) shear span-to-depth ratio (a/d). For each parameter, the predicted response curves are plotted for the load-deflection and load-steel strain relations. The control specimen used in the parametric studies, is the corbel with constant depth A3 with the geometry and material properties given in Table 1.

4.1. Evaluation criteria of the parametric studies

From the predicted load-deflection and load-steel strain curves for corbels, the effects of the analyzed parameters have been studied using the following measures:

- Loads at the yield level (P_y) and at the ultimate level (P_u).
- Deflection at the yield level (Δ_y) and at the ultimate level (Δ_u).
- Displacement ductility (μ_Δ) = (Δ_u/Δ_y).
- Toughness (I) = the area under the load-deflection curve.
- Strain ductility (μ_s) = ultimate steel strain (ε_u)/yield strain (ε_y).

For the given parameters, the results of a specified specimen are considered as reference values to calculate the following relative measures:

$$Q_{yR} = \frac{P_y}{P_{yr}} \tag{17}$$

$$Q_{uR} = \frac{P_u}{P_{ur}} \tag{18}$$

$$\alpha_{yR} = \frac{\Delta_y}{\Delta_{yr}} \tag{19}$$

$$\alpha_{uR} = \frac{\Delta_u}{\Delta_{ur}} \tag{20}$$

$$I_{uR} = \frac{I}{I_{ur}} \tag{21}$$

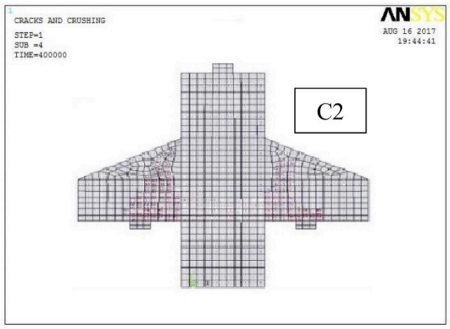

(a) C2 - Predicted Crack Pattern

(b) C2- experimental Crack Pattern

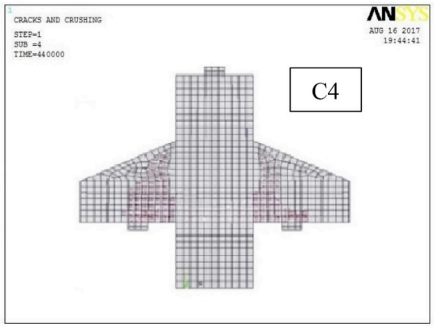

(c) C4 - Predicted Crack Pattern

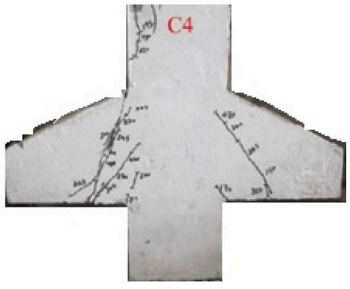

(d) C4- experimental Crack Pattern

Fig. 13. Predicted and observed cracking patterns for corbels (C2) and (C4).

Table 2
Comparison of the experimental results with NLFEA by ANSYS software.

Corbel	P_y (EXP) kN	P_u (EXP) kN	P_y (FE) kN	P_u (FE) kN	Δ_y (EXP) mm	Δ_u (EXP) mm	Δ_y (FE) mm	Δ_u (FE) mm	$\frac{P_{y(EXP)}}{P_{y(FE)}}$	$\frac{P_{u(EXP)}}{P_{u(FE)}}$	$\frac{\Delta_{y(EXP)}}{\Delta_{y(FE)}}$	$\frac{\Delta_{u(EXP)}}{\Delta_{u(FE)}}$	$\frac{I_{(EXP)}}{I_{(FE)}}$	*Failure Mode*
SP.23	125	126.5	118	123	3.45	5.57	3.10	5.4	1.06	1.02	1.11	1.06	0.99	F
SP.37	133	140	120	129.5	1.87	5.4	1.64	5.2	1.10	1.08	1.14	1.04	1.06	F
A2	90	98	87.5	92.5	1.30	5.4	1.10	5.32	1.028	1.06	1.18	1.02	0.98	F
A3	100	104.5	92	101	1.30	10.06	1.20	10	1.086	1.035	1.083	1.006	1.03	F
C2	175	198	174.5	200	1.80	2.3	1.79	2.52	1.003	0.99	1.005	0.91	0.94	D.S
C4	165	250	175	270	1.60	2.4	1.55	2.55	0.942	0.925	1.032	0.94	0.93	D.S
C1-SF	2417	3282	2530	3230	0.92	2.1	0.82	2.2	0.955	1.016	1.12	0.95	0.97	D.S
C2-SF	2012	2408	2350	2520	0.85	2.47	1.0	2.28	0.86	0.955	0.85	1.08	1.012	D.S
Average									1.01	1.01	1.08	1.01	1.00	
Standard deviation									0.08	0.05	0.10	0.07	0.05	
Coefficient of variation									7.65%	4.80%	9.57%	6.54%	4.94%	

Where:
P_y: load at yielding of steel reinforcement (kN).
P_u: ultimate load (kN).
Δ_y: the deflection at the yielding (mm).
Δ_u: the deflection at the ultimate(mm).
I: the toughness (the area under the load-deflection curve).
F: flexural failure.
D.S: diagonal shear.

Where:

Q_{yR} = shear capacity ratio at the yield load level.
P_{yr} = shear capacity at the yield load level for the control specimen.
Q_{uR} = shear capacity ratio at the ultimate load level.
P_{ur} = shear capacity at the ultimate load level for the control specimen.
α_{yR} = deflection ratio at the yield load level.
Δ_{yr} = deflection at the yield load level for the control specimen.
α_{uR} = deflection ratio at the ultimate load level.
Δ_{ur} = deflection at the ultimate level for the control specimen.
I_{uR} = toughness ratio.
I_{ur} = toughness of the control specimen.

Table 4 presents a summary of the analysis results of parametric studies.

4.2. Effect of concrete strength

Three SFRC corbels are analyzed with different concrete compressive strengths (f_c') (30, 40 and 52.9 MPa) for (S1, S2 and S3) respectively. The load-deflection curves and the load-steel strain curves for the

Table 3
The input parameters for the analyzed specimens in parametric studies.

Corbel	f_c, MPa	V_f %	$\frac{l_f}{\varphi_f}$	$\rho_h = A_h/(bd)$ %	a/d	Studied Parameter
S1	30	1.0	60	–	0.928	f_c
S2	40	1.0	60	–	0.928	
S3	52.9	1.0	60	–	0.928	
S4	52.9	0.0	–	–	0.928	V_f
S5	52.9	0.5	60	–	0.928	
S6	52.9	1.0	60	–	0.928	
S7	52.9	1.0	0.0	–	0.928	$\frac{l_f}{\varphi_f}$
S8	52.9	1.0	50	–	0.928	
S9	52.9	1.0	100	–	0.928	
S10	48.5	–	–	–	0.928	ρ_h
S11	48.5	–	–	1.77	0.928	
S12	48.5	–	–	4.90	0.928	
S13	52.9	1.0	60	–	0.5	a/d
S14	52.9	1.0	60	–	0.7	
S15	52.9	1.0	60	–	0.928	

analyzed specimens are plotted in Fig. 14. The comparison between the given results indicates that increasing f_c' leads to an enhancement in shear capacity (V_u) by 27% and 45% for specimens S2 and S3 when compared to S1. Also, it increases the longitudinal steel strain (ε_s) for corbels S2 and S3 respectively by 70% and 84% compared to specimen S1. The calculated strain ductility (μ_s) is 1.2, 4 and 7 for S1, S2 and S3 respectively. Then, the strain ductility (μ_s) has been increased due to increase the concrete compressive strength (f_c'). Significant enhancement in the toughness (I) which calculated as the area under the load-deflection curve is observed due to the increase of f_c'. Toughness is enhanced by 54% and 107% for specimens S2 and S3 respectively compared to specimen S1. Finally, the crack patterns are shown in Fig. 15 for S1, S2 and S3. It is found that increasing (f_c') delays the possibility of premature shear failure for SFRC corbels.

4.3. Effect of volume of steel fibers

Three SFRC corbels with different fiber volume (V_f) are analyzed. The fiber volumes are considered as (0.0%, 0.5% and 1.0%) respectively for corbels (S4, S5 and S6). Fig. 16 shows the predicted response curves for the specimens. An enhancement in the shear capacity (V_u) by 15% and 31% has been observed for specimen S5 and S6 respectively when compared with S4. Also, significant improvement in the toughness (I) and strain ductility (μ_s) is noticed. The predicted increase in the toughness (I) is 171% and 513% for specimens S5 and S6 respectively compared to specimens. The predicted values of strain ductility (μ_s) are 3.5, 6, and 7 for specimens S4, S5 and S6 respectively. The strain of the tension reinforcement (ε_s) is enhanced by providing higher fiber volume (V_f). As clarified in the load-steel strain curves, ε_s is enhanced for specimens S5 and S6 by 73% and 102% respectively compared to specimen S4. The predicted crack patterns are shown in Fig. 17 for

Table 4
The output results for the analyzed specimens of parametric studies.

Corbel	P_y kN	P_u kN	Δ_y mm	Δ_u mm	Q_{yR}	Q_{uR}	α_{yR}	α_{uR}	μ_Δ	μ_s	I	I_{uR}
S1	65.0	69.5	0.98	6.95	1.00	1.00	1.00	1.00	7.10	1.20	460	1.00
S2	84.0	88.0	1.09	8.55	1.29	1.27	1.11	1.23	7.80	4.0	710	1.54
S3	92.0	101.0	1.12	10.0	1.42	1.45	1.14	1.44	8.90	7.0	954	2.07
S4	68.0	77.0	1.05	2.54	1.00	1.00	1.00	1.00	2.40	3.50	153	1.00
S5	72.0	88.5	1.10	5.40	1.07	1.15	1.05	2.13	4.90	6.0	415	2.71
S6	92.0	101.0	1.12	10.0	1.36	1.31	1.07	3.94	8.90	7.0	954	6.24
S7	67.5	77.0	1.05	2.54	1.00	1.00	1.00	1.00	2.40	3.50	153	1.00
S8	92.0	101.0	1.12	10.0	1.36	1.31	1.06	3.94	8.90	7.0	954	6.24
S9	94.0	104.0	1.14	15.0	1.39	1.35	1.08	5.90	13.20	9.80	1482	9.69
S10	67.5	77.0	1.05	2.54	1.00	1.00	1.00	1.00	2.40	3.50	153	1.00
S11	87.5	92.5	1.10	5.32	1.30	1.20	1.05	2.10	4.80	6.50	450	2.94
S12	100.0	102.5	1.13	9.55	1.48	1.33	1.08	3.76	8.50	7.80	936	6.12
S13	148.0	158.0	0.84	8.40	1.00	1.00	1.00	1.00	10.0	15.0	1218	1.00
S14	127.0	132.0	1.02	9.20	0.86	0.84	1.21	1.10	9.0	12.0	1170	0.96
S15	92.0	101.0	1.12	10.0	0.62	0.64	1.33	1.20	8.90	7.0	954	0.78

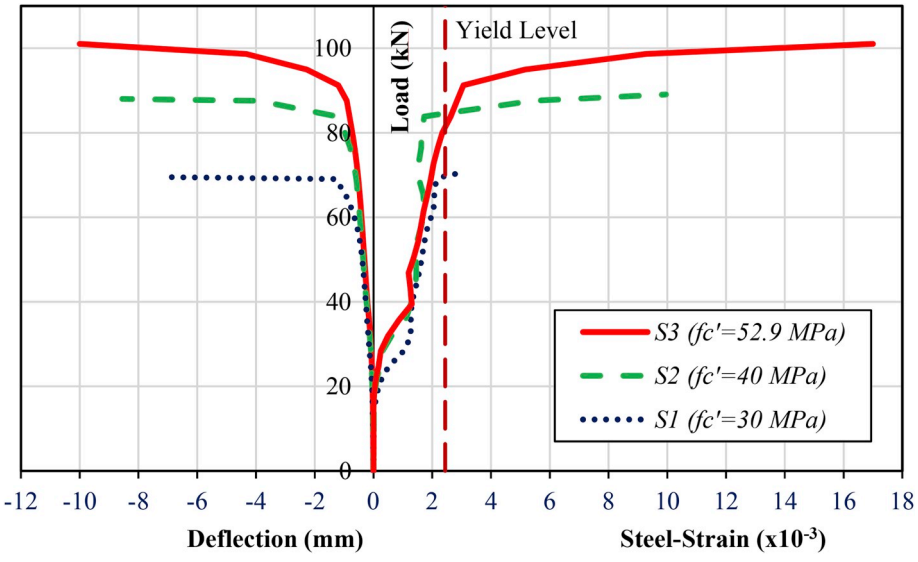

Fig. 14. Predicted response curves for corbels S1, S2 and S3.

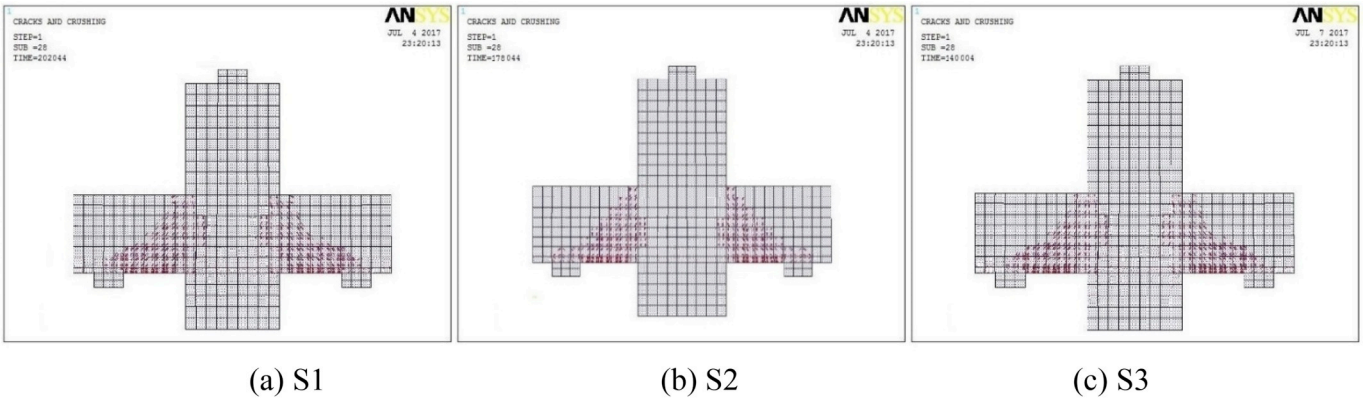

Fig. 15. Crack patterns for corbel S1, corbel S2 and corbel S3.

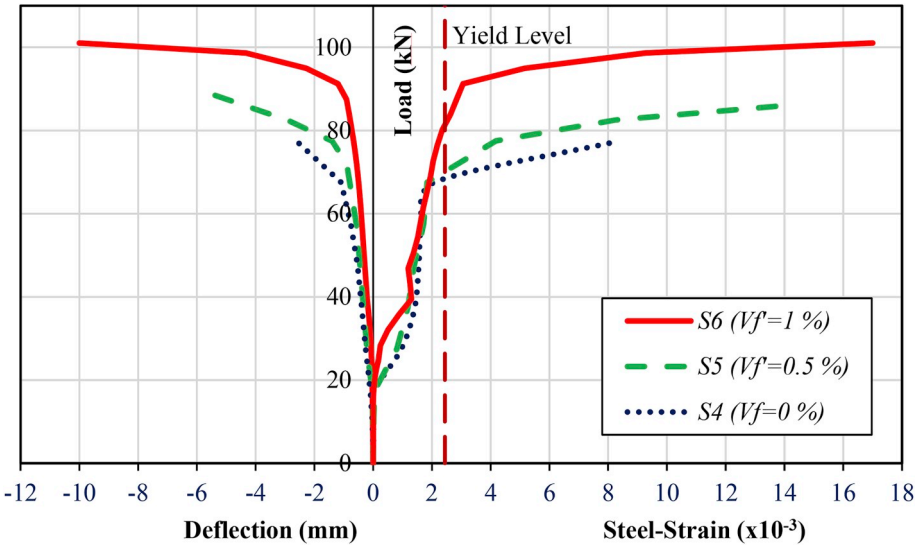

Fig. 16. Predicted response curves for corbels S4, S5 and S6.

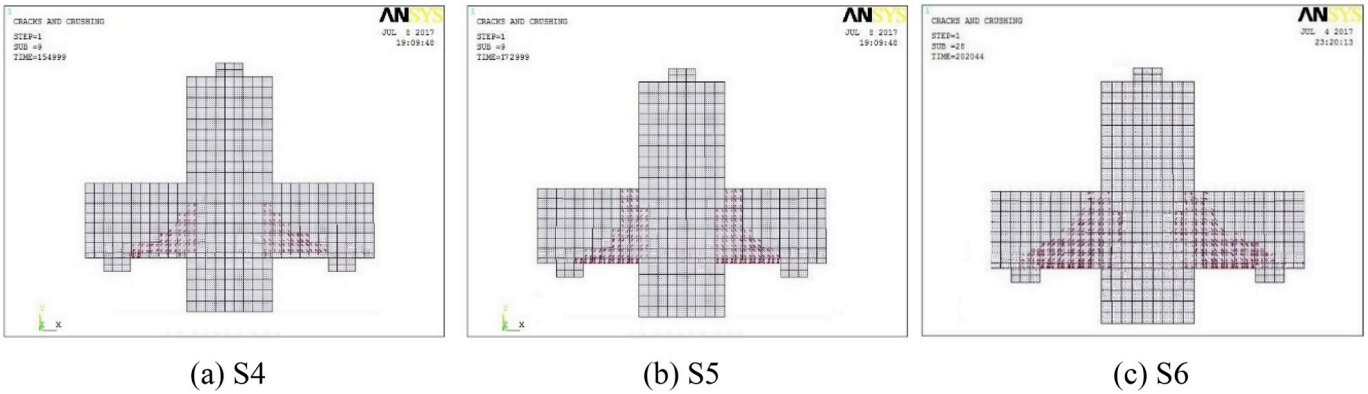

Fig. 17. Crack patterns for corbel S4, corbel S5 and corbel S6.

specimens S4, S5 and S6. Increasing fiber volume delays premature shear failure for corbels and increases cracks propagation at corbel length and depth.

4.4. *Effect of fiber aspect ratio*

Three SFRC corbels having different fiber aspect ratio (l_f/φ_f) are considered. The studied fiber aspect ratios are 0, 50 and 100 respectively for specimens (S7, S8 and S9). The predicted load-deflection and load-steel strain curves for the specimens are plotted in Fig. 18. It is clear that increasing (l_f/φ_f) improves shear capacity V_u of the specimens by 30% and 36% for S8 and S9 with respect to S7. Furthermore, great enhancement in the toughness (I) is observed 523% and 868% for specimens S8 and S9 respectively when compared to S7. Also, the strain in the tension steel (ε_s) is increased by 102% and 185% for specimens S8 and S9 compared to the reference specimen S7. The strain ductility (μ_s)

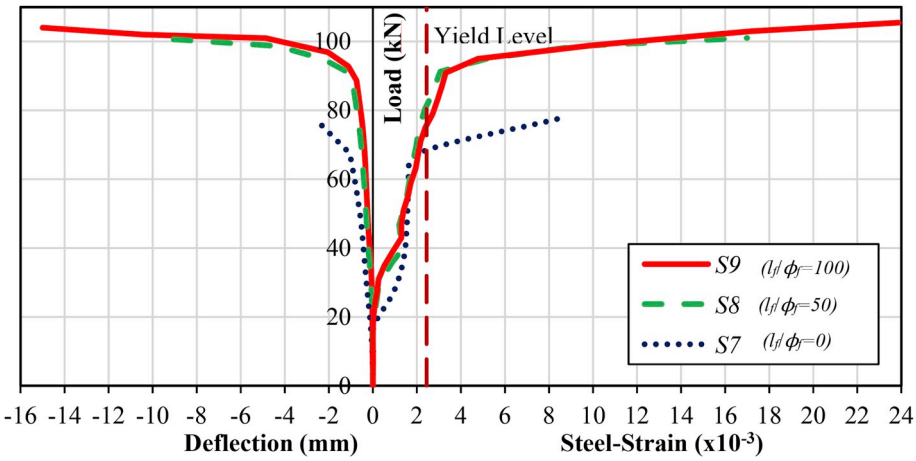

Fig. 18. Predicted response curves for corbels S7, S8 and S9.

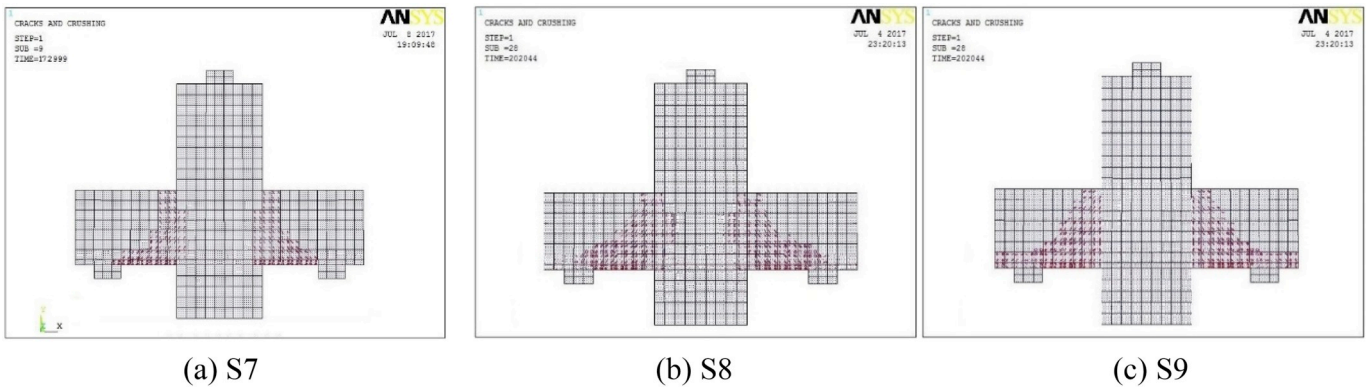

Fig. 19. Crack patterns for corbel S7, corbel S8 and corbel S9.

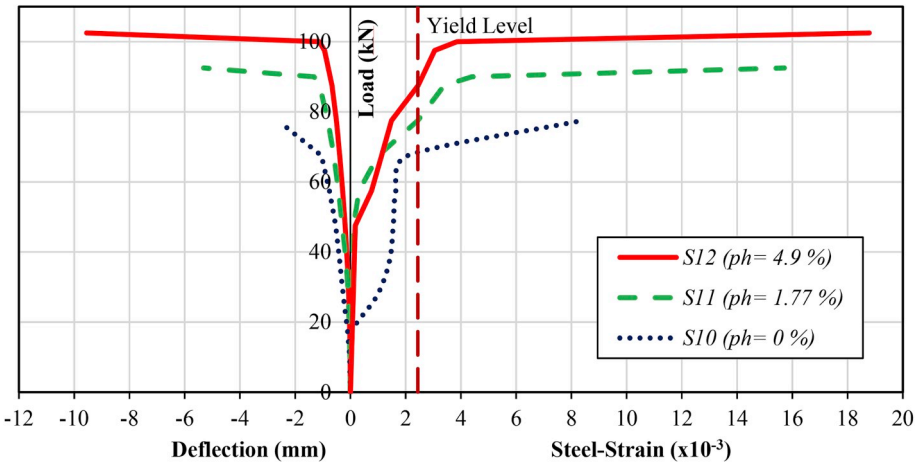

Fig. 20. Predicted response curves for corbels S10, S11 and S12.

is improved by increasing (l_f/φ_f). The estimated values of (μ_s) are 3.5, 7, and 9.8 for S7, S8 and S9 respectively. The crack patterns for the specimens are shown in Fig. 19 for corbels S7, S8 and S9 respectively. Increasing fiber aspect ratio spreads cracks more widely and gradually along the span and depth of corbel.

4.5. *Effect of ratio of the horizontal stirrups*

Three corbels with different horizontal stirrups ratio (ρ_h) has been investigated. The corbels are denoted by S10, S11 and S12 and are reinforced with (ρ_h) as 0.0%, 1.77% and 4.90% respectively. Fig. 20 present the predicted response curves for the analyzed specimens. An enhancement in the shear capacity (V_u) is predicted for specimens S11 and S12 by 20% and 33% respectively when compared to specimen S10. With respect to S10, significant improvement in the toughness (I) and strain ductility (μ_s) is noticed. The predicted increase in the toughness (I) is 194%, and 511% for specimen S11 and S12 respectively. The predicted values of strain ductility are 3.5, 6.5, and 7.8 for specimens S10,

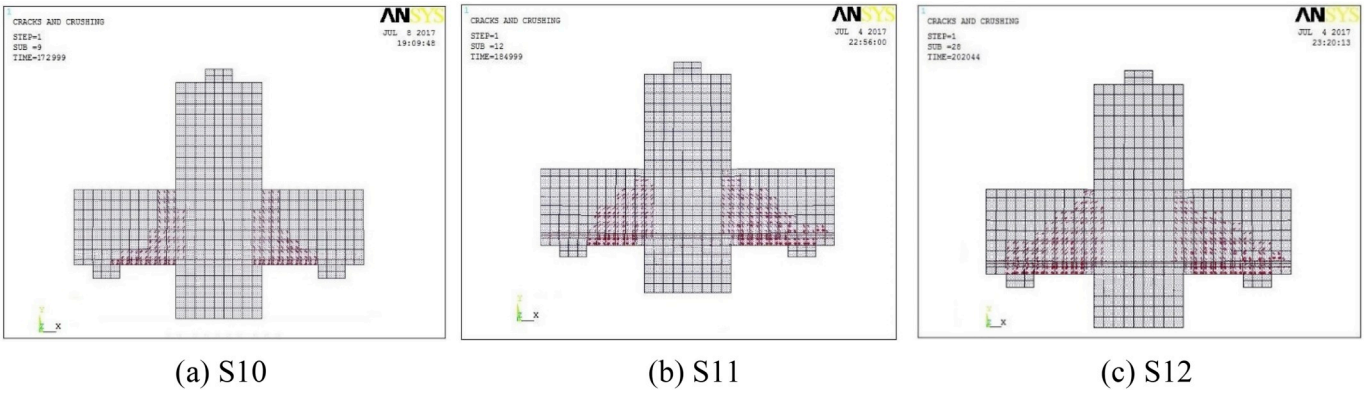

Fig. 21. Crack patterns for corbel S10, corbel S11 and corbel S12.

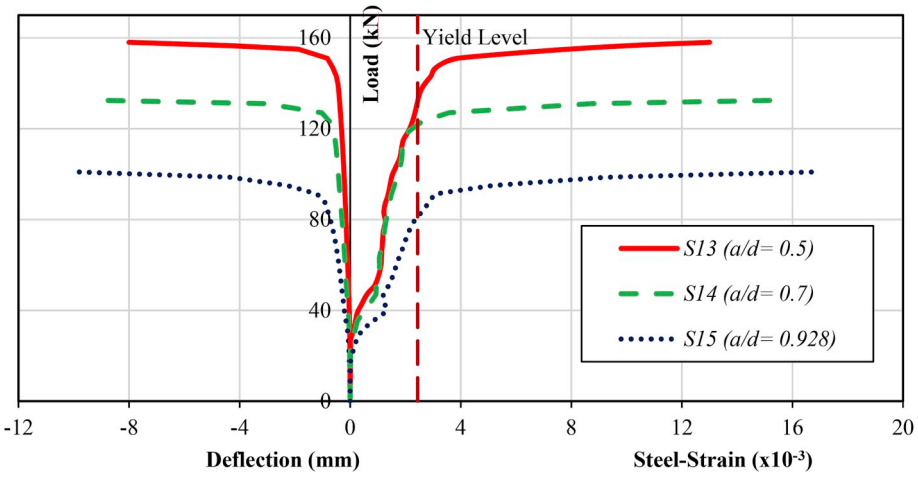

Fig. 22. Predicted response curves for corbels (S13, S14 & S15).

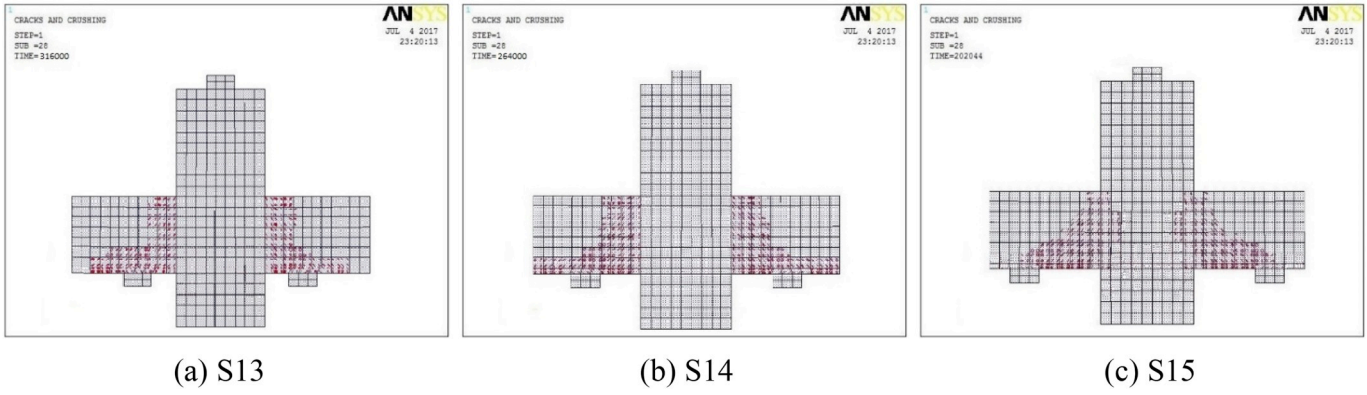

Fig. 23. Crack patterns for corbel S13, corbel S14 and corbel S15.

S11 and S12 respectively. Increasing the ratio of the horizontal stirrups increases the main steel strain (ε_s). As shown in the load-steel strain curves, the increased ratio of the horizontal stirrups for corbels S11 and S12 increases ε_s by 87.5% and 124% respectively. Fig. 21 shows the crack patterns of the analyzed corbels (S10, S11 and S12). It is predicted that increasing the horizontal stirrups ratio delays premature shear failure occurrence and leads to more spreading in cracks through the corbel length and depth.

4.6. Effect of shear span to depth ratio

Three SFRC corbels are studied with different shear span to depth ratio (a/d) values. The used shear – span to depth ratios are 0.5, 0.7 and 0.928 for specimens S13, S14 and S15 respectively. The predicted response curves for the specimens are plotted in Fig. 22. Generally, increasing (a/d) reduces the shear capacity (V_u) of the corbel. Increasing (a/d) for specimens S14 and S15 by 40% and 86% decreases V_u by 16% and 36% respectively. Increasing (a/d) decreases slightly the toughness (I). As shown in the load-deflection curves, the toughness is decreased for specimens S14 and S15 by 4% and 22% respectively. As shown in

load-steel strain curves, the steel strain (ε_s) is increased for specimens S14 and S15 by 20% and 31% respectively. Also, the strain ductility (μ_s) is increased by increasing (a/d). The values of (μ_s) are 5.5, 6.5, and 7 for S13, S14 and S15 respectively). The cracking patterns of the SFRC corbels (S13, S15 and S15) are also shown in Fig. 23. The amount of vertical and inclined cracks increases with the increase of (a/d) ratio.

5. Conclusions

From the validation and parametric studies of the finite element computer program ANSYS, the following conclusive points are drawn:

(1) For all case studies, the predictions of the load-deflection response as well as the cracking patterns and the failure modes using the nonlinear FE program (ANSYS) and the proposed constitutive models showed a good agreement with the experimental results. At yield level, the overall average for [$P_{y\ (EXP)}/P_{y\ (FE)}$] ratio and [$\Delta_{y\ (EXP)}/\Delta_{y\ (FE)}$] ratio is 1.01 and 1.08 respectively. At the ultimate level, the overall average for [$P_{u\ (EXP)}/P_{u\ (FE)}$] ratio and [$\Delta_{u\ (EXP)}/\Delta_{u\ (FE)}$] ratio for all specimens are 1.01, 1.01 respectively.
(2) Increasing concrete compressive strength (f_c') enhances the corbel shear capacity (V_u) and the toughness (I). The use of corbel with $f_c' = 40$ MPa and 52.9 MPa improves shear capacity by 27% and 45% respectively and enhances the toughness by 54% and 107% respectively compared to corbel with $f_c' = 30$ MPa.
(3) The inclusion of the steel fibers in the corbels improve the shear capacity and the strain ductility. Using concrete with fiber volume (V_f) 0.5% and 1% improves the shear capacity by 15% and 31% respectively compared to corbel without fibers. In addition, the strain ductility (μ_s) is increased by 72% and 100% when compared with non-fibrous corbel. Finally, the optimal fiber volume content for design applications of SFRC corbels is 1–2%.
(4) The horizontal stirrups (ρ_h) enhance the performance of SFRC corbels, compared with corbel without horizontal stirrups, and significant improvement in toughness (I) is predicted by 194% and 512% for corbels with (ρ_h) = 1.7% and 4.9% respectively. Also, the corbel ultimate shear strength is improved by 20% and 32.5% compared to corbel without (ρ_h).
(5) Increasing the shear span-to-depth ratio (a/d) reduces the corbel ultimate shear capacity and toughness. Using corbels with (a/d) = 0.7 and 0.928 decreases the shear capacity by 16% and 36% respectively and reduces the toughness by 4% and 22% respectively when compared to corbels with (a/d) = 0.5.

Author statement

F.B.A. Beshara: Conceptualization, Methodology, Supervision, Writing - Review & Editing.
T.S. Mustafa: Conceptualization, Methodology, Supervision, Writing - Review & Editing, Software.
A.A. Mahmoud: Conceptualization, Methodology, Supervision, Writing - Review & Editing.
M.M.A. Khalil: Software, Validation, Writing, Data Curation.

Declaration of competing interest

The authors declare that they have no conflict of interest.

Appendix A. Supplementary data

Supplementary data to this article can be found online at https://doi.org/10.1016/j.jobe.2019.101092.

References

[1] N.I. Fattuhi, Strength of SFRC corbels subjected to vertical load, J. Struct. Eng. ASCE 116 (3) (1990) 701–718.
[2] G. Campione, L. LaMendola, M. Papia, Flexural behavior of concrete corbels containing steel fibers or wrapped with FRP sheets, Mater. Struct. 38 (6) (2005) 617–625.
[3] M. Salman, I. Al-Shaarbaf, Experimental study on the behavior of normal and high strength self-compacting reinforced concrete corbels, J. Eng. Dev. 18 (No.6) (2014).
[4] M. Alameer, Effects of Fibers and Headed Bars on the Response of Concrete Corbels,, MSc Thesis, Department of Civil Engineering and Applied Mechanics McGill University, Montreal, Canada, May 2004.
[5] N.I. Fattuhi, Strength of (FRC) corbels in flexure, J. Struct. Eng. 120 (2) (February, 1994) 360–377.
[6] N.I. Fattuhi, P. Hughes, Reinforced steel fiber concrete corbels with various shear span-to-depth ratio, ACI Struct. J. 86 (6) (October, 1990) 590–596.
[7] R. Heather, Y. Hossien, D. Michael, B. Oguzhan, Investigation of corbels designed according to strut-and- tie and empirical methods, ACI Struct. J. 115 (3) (2018) 17–183.
[8] M. Maha, T. Nagham, M. Milad, Ultra-high performance steel fibers concrete corbels: experimental investigation, Case Stud.Constr. Mater. vol. 7 (2017) 180–190.
[9] S. Lliyas, W. Abhijeet, N. Deepak, Investigation of steel fiber reinforced concrete corbels by experimental and analytical method, Int. J. Concr. Technol. 2 (2) (2016) 23–29.
[10] J.M. Yang, Influence of Steel Fibers and Bars on the Serviceability of High-Strength Concrete Corbels, ASCE. J., 2012, pp. 123–129.
[11] S. Kumar, S.V. Barai, "Neural Networks Modelling of Shear Strength of SFRC Corbels without Stirrups", Applied Soft Computing vol. 6, ElSevier, 2010, pp. 135–148.
[12] N.I. Fattuhi, Ductility of reinforced concrete corbels containing either steel fibers or stirrups, ACI Struct. J. 86 (6) (December, 1989) 644–651.
[13] G. Campione, Performance of steel fibrous reinforced concrete corbels subjected to vertical and horizontal loads, J. Struct. Eng. ASCE (May 2009) 519–529.
[14] A. Cevik, E. Kurtoglu, Stochastic finite element based reliability analysis of steel fiber reinforced concrete (SFRC) corbels, J. Comp. Concr. 15 (No. 2) (2015) 1–20.
[15] M. Rezaei, S.A. Osman, N.E. Shanmugam, Primary and Secondary Reinforcements in Corbels under Combined Action of Vertical and Horizontal Loadings, International Conference on Composite Structures, Porto, 2011, pp. 1–10.
[16] G. Danying, Z. Junwei, Finite Element Analysis of Shear Behaviors for Steel Fiber Reinforced Concrete Corbels by ANSYS, Second International Conference on Computer Modelling and Simulation, 2010.
[17] M.M.A. Khalil, Analytical Studies on Steel Fiber Reinforced Concrete Corbels, MSc Thesis, Benha University, Faculty of Engineering, Shoubra, Egypt, 2018.
[18] ANSYS–Release Version 12.1.0, A Finite Element Computer Software and User Manual for Nonlinear Structural Analysis, ANSYS Inc. Canonsburg, , PA., 2009.
[19] E. Montoya, F. Vecchio, S.A. Sheikh, Compression field modelling of confined concrete, J. Struct. Eng. Mech. 12 (3) (2001).
[20] ACI Committee 318, Building Code Requirements for Structural Concrete ACI, vols. 318–14, 2014.
[21] P. Soroushian, C.D. Lee, Constitutive modelling of steel fiber reinforced concrete under direct tension and compression, in: Proceeding of the International Conference on Recent Development in Fiber Reinforcement Cement and Concrete, Cardiff, U.K., 1989, pp. 363–377.
[22] T.S. Mustafa, Behavior of High Strength Fiber Reinforced Concrete Beams, MSc Thesis, Benha University, Faculty of Engineering, Shoubra, Egypt, 2007.
[23] A. Abdul-Razzak, A. Mohammed, Modelling and numerical simulation of high strength fiber reinforced concrete corbels, Appl. Math. Model. 35 (2011) 2901–2915.
[24] A. Demeke, I. Tegos, Steel fiber reinforced concrete in biaxial stress tension compression conditions, ACI Struct. J. 91 (5) (September 1994) 579–584.
[25] S.J. Foster, A.R. Malik, Evaluation of efficiency factor models in strut and tie modelling of non-flexural members, ASCE, J. Struct. Eng. 128 (5) (2002) 569–577. May.
[26] Eurocode 3, Design of Steel Structures, ENV EC3 Part 1.2, Eurocode, 2005.